FDM Printing: a Fabrication Method for Fluidic Soft Circuits?

Savita V. Kendre, 1,† Lehong Wang, 1,2,† Ethan Wilke, 1 Nicholas Pacheco, 1 Loris Fichera, 1,3 and Markus P. Nemitz 1,4,5

Abstract—Existing fluidic soft logic gates for controlling soft robots typically depend on labor-intensive manual fabrication or costly printing methods. In our research, we utilize Fused Deposition Modeling to create fully 3D-printed fluidic logic gates, fabricating a valve from thermoplastic polyurethane. We investigate the 3D printing of tubing and introduce a novel extrusion nozzle for tubing production. Our approach significantly reduces the production time for soft fluidic valves from 27 hours using replica molding to 3 hours with FDM printing. We apply our 3D-printed valve to develop optimized XOR gates and D-latch circuits, presenting a rapid and cost-effective fabrication method for fluidic logic gates that aims to make fluidic circuitry more accessible to the soft robotics community.

I. INTRODUCTION

Soft robots, fabricated from compliant materials, offer shape adaptability, safer human interactions, and high-impact resilience compared to traditional robots [1]. Despite their pneumatic actuation [2], many soft robots still rely on rigid electronic control system like solenoid valves and microcontrollers, compromising system compliance. To mitigate this issue, flexible electronics is increasingly integrated into soft robotic designs [3]. Advances in fluidic control have also enabled complex motion patterns and circuit designs [4], [5]. Silicone-based soft fluidic valves have emerged as versatile elements for fluidic control, capable of performing tasks like pressure switching and sensing [6]. These valves have been used in applications like soft crawlers and robotic grippers [6], [7]. They can also be configured into various logic gates and circuits, including NOT-gates, AND-gates, OR-gates, S-R latches, D-type latches, 2-bit shift registers, and ring oscillators [8], [9]. With some design adaptations, these devices can serve as memory elements to store information [10]. Soft ring oscillators have been used to create a turtle-like, soft-legged robot generating oscillating signals analogous to biological central pattern generators [11].

The incorporation of soft fluidic valves in soft robotic control systems has catalyzed efforts toward economical,

This work was supported by the National Science Foundation under CAREER Grant No. 2237506.

Corresponding author: Markus P. Nemitz, mnemitz@wpi.edu

- † Indicates equal contribution
- ¹Department of Robotics Engineering, Worcester Polytechnic Institute, Worcester, MA 01609, USA
- ²Department of Computer Science, Worcester Polytechnic Institute, Worcester, MA 01609, USA
- ³Department of Biomedical Engineering, Worcester Polytechnic Institute, Worcester, MA 01609, USA
- ⁴Department of Mechanical and Materials Engineering, Worcester Polytechnic Institute, Worcester, MA 01609, USA
- ⁵Department of Electrical and Computer Engineering, Worcester Polytechnic Institute, Worcester, MA 01609, USA

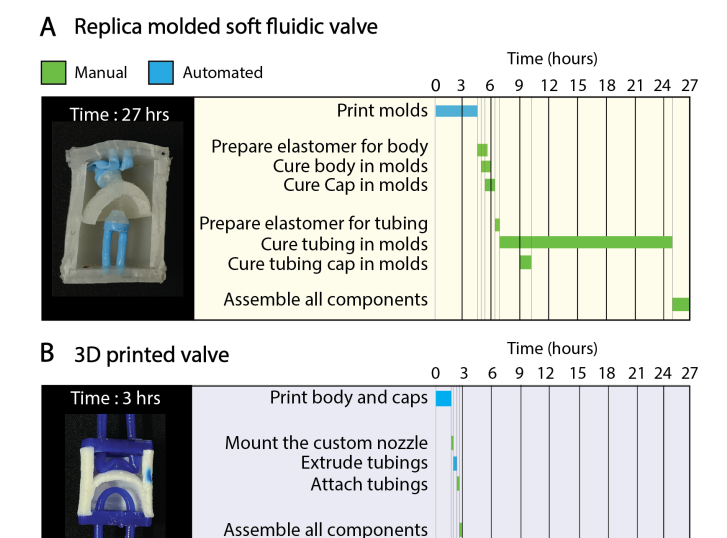


Fig. 1. Comparison of replica molding and FDM printing of a soft fluidic valve. The time required for fabricating the soft fluidic valve is compared between A) replica molding and B) FDM printing. The fabrication time is reduced from 27 hours to 3 hours when using 3D printing.

automated design architectures. Using commercially available materials, recent work has demonstrated tube balloon logic devices, buckling-sheet inverters, logic-enabled textiles, as well as fluidic computation kits as cost-efficient control modalities [12]-[16]. However, these techniques predominantly rely on labor-intensive, manual fabrication processes that are susceptible to operator-induced errors and component variations. As an alternative, additive manufacturing techniques like 3D printing have been employed to develop control elements such as complementary fluidic circuits, tunable soft fluidic valves, and fluidic diodes and transistors [5], [17], [18]. The recent introduction of Eulerian path printing permits the fabrication of airtight actuators and control elements using Fused Deposition Modeling (FDM) with custom filaments [19]. Despite progress in automating cost-effective fabrication techniques, the necessity for expensive printers and specialized filaments constitutes a financial obstacle to widespread replication across the global academic community.

Our work is inspired by the soft fluidic valve from Rothemund et al. due to its multi-functionality (AND-, OR-, and NOT-gate configurations) for soft robotic systems [6]. Comprising a cylindrical body segmented by a snapping hemispherical membrane, the valve features two chambers connected by top and bottom tubing to the membrane and

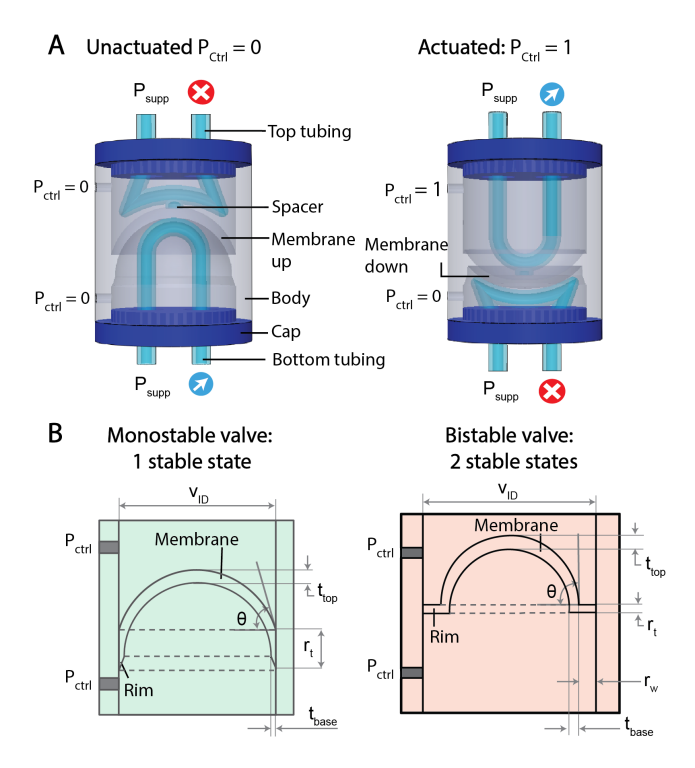
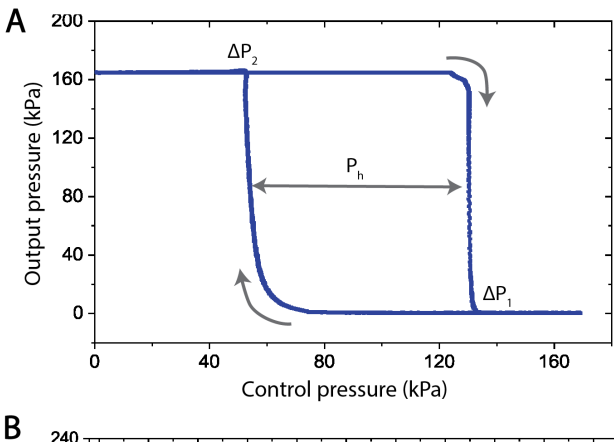


Fig. 2. **The 3D printed valve.** (A) The schematic shows components of the valve and it's operation in both actuated and un-actuated states. (B) The CAD drawing shows the influential parameters and monostable and bistable designs of the 3D printed valves.

end caps. A pressure differential between these chambers triggers the membrane to snap, thereby kinking one tube while un-kinking the other. This operation is functionally analogous to a complementary metal-oxide-semiconductor (CMOS) technology.

The soft fluidic valve is fabricated using replica molding. Silicone rubber or similar elastomers are injected into molds and cured. This fabrication process takes up to 27 hours to create a single valve (**Figure 1A**). While cost-effective for mass production, this method is time-intensive for prototyping and iterative designs. Each iteration involves mold redesign, 3D printing, pouring materials, and solidifying the silicone rubber, making it both laborious and time-consuming. Detailed fabrication steps for creating a silicone-based soft fluidic valve are available on our GitHub repository (https://github.com/roboticmaterialsgroup/soft-fluidic-valve).

Overall, the widespread adaptation of current fluidic circuits are hindered by either labor-intensive manual processes or costly automated machinery. To address these challenges, we chose the soft fluidic valve as a reference design and probed cost-effective, automated fabrication process via FDM printing—a method noted for its affordability and wide range of materials [20]. This approach resulted in a reduction of the fabrication time to 3 hours (**Figure 1B**). Our research question is: Can FDM printing effectively fabricate complementary logic gates using low-cost printers and commercially available thermoplastic polyurethanes? To this end, we explore the viability of 3D printing a soft fluidic



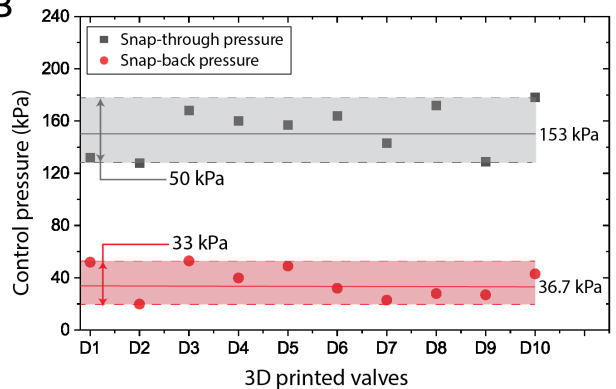


Fig. 3. Characterization of the 3D printed valve. (A) The plot shows the relationship between the control pressure and the output pressure for the bottom tubing. (B) The shaded region indicates the total observed range for snap-through and snap-back pressures for 3D printed valves (N = 10).

valve employing a Prusa MK3S printer (\$649) and Filaflex 60A filament. The key contributions of this work include:

- Design and fabrication of an entirely FDM-printable soft fluidic valve.
- Reduction of the fabrication time from 27 hours with replica molding to 3 hours using FDM printing.
- Study and comparison of 3D printed tubing.
- Introduction of a novel, custom-made 3D printing nozzle for the direct extrusion of tubing.
- Demonstration of our FDM-printable soft fluidic valves as a optimized XOR gate and a D-latch circuit.

II. THE 3D PRINTED VALVE

Our 3D-printed valve features a body with an integrated membrane, top and bottom tubing, and the end caps. In an unactuated state, the top and bottom chambers are at 0 kPa pressure ($P_{ctrl} = 0$), the top tubing is kinked, inhibiting airflow, while the bottom tubing remains open, facilitating airflow (**Figure 2A**). Upon application of positive pressure of 153 kPa ($P_{ctrl} = 1$) to the top chamber, the membrane undergoes a downward snapping motion. This action unkinks the top tubing, allowing airflow, while kinking the bottom tubing, blocking airflow. This dynamic mimics the behavior of a CMOS technology, improving the energy efficiency of fluidic switching compared to NMOS (n-

channel metal-oxide-semiconductor) or PMOS (p-channel metal-oxide-semiconductor) devices.

We categorized the soft fluidic valve into monostable and bistable designs (**Figure 2B**). In this context, a monostable design has a single stable state and requires sustained control pressure for actuation. Whereas, a bistable design has two stable states and retains its position even after removal of control pressure. Typically, bistable designs are employed for memory elements while monostable designs are used for constructing logic gates. To investigate the parameters affecting stability, we examined membrane top and base thickness (t_{top} , t_{base}), angle (θ), rim dimensions (r_t , r_w), and the inner diameter of the valve (V_{ID}) as these factors critically determine the stability of the valve. We provide the parametric values for both monostable and bistable designs (**Table I**).

We studied the relationship between the control pressure and the resulting output pressure (**Figure 3A**). In our experiments, we applied a constant supply pressure ($P_{supp} = 160 \text{ kPa}$) to the lower tubing, and atmospheric pressure to the upper tubing. We successively increased the control pressure in the valve of the top chamber, while maintaining the bottom chamber at atmospheric pressure. This resulted in the membrane experiencing a snap-through at an average pressure of 153 kPa (ΔP_1), effectively sealing the lower tubing. Upon pressure reduction, a snap-back occurred at 56 kPa (ΔP_2), reopening the lower tubing. The hysteresis of the valve reveals susceptibility to a pressure disturbance ($P_h = 78 \text{ kPa}$) in the system. All plots are based on the monostable design of the 3D printed valve.

We assessed the reproducibility of snap-through and snap-back pressures in ten 3D-printed valves **(Figure 3B)**. The shaded areas indicate the observed maximum deviations—50 kPa for snap-through and 33 kPa for snap-back pressures—leading us to advise actuating the valves at 153 kPa. Importantly, this variability may stem from several sources, such as printer model, filament properties, and printing conditions, underscoring the necessity for rigorous standardization of these parameters to ensure consistent, high-quality outputs.

For 3D printing the soft fluidic valve with economical

TABLE I The values of geometrical parameters for monostable and bistable designs of the 3D printed valve

Parameters	Monostable design	Bistable design
Membrane top thickness (t _{top})	1.4 mm	1.6 mm
Membrane base thickness (t _{base})	0.6 mm	1.2 mm
Angle (θ)	75 deg.	90 deg.
Rim thickness (r _t)	4 mm	1 mm
Rim width (r _w)	0 mm	2 mm
Valve inner dia. (V _{ID})	16 mm	20 mm

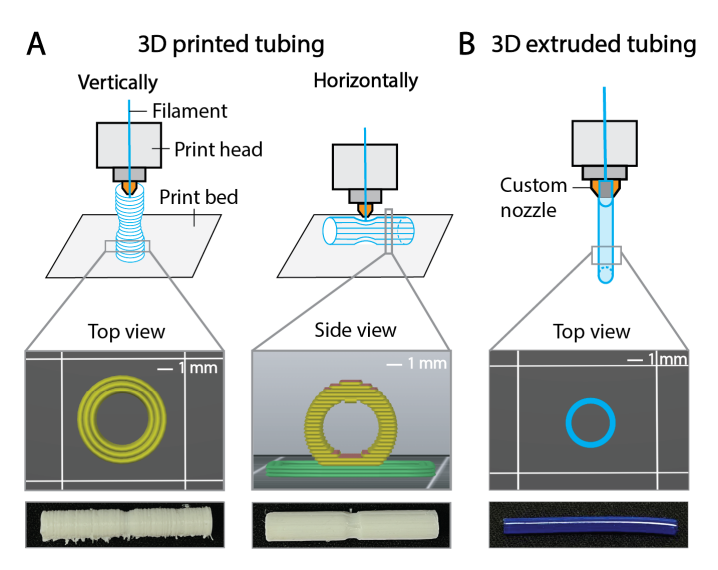


Fig. 4. **FDM printed and extruded tubing.** (A) The hourglass-shaped tubing is printed both vertically and horizontally. Vertically printed tubing breaks easily due to weak layer bonding, whereas horizontally printed tubing exhibits the staircase effect, leading to minor leakage during kinking. (B) We use our custom nozzle to directly extrude tubing using thermoplastic filaments, resulting in a homogeneous strong layer bonding and increased durability.

FDM printers, we segmented the valve into three fundamental elements: the body, caps, and tubing.

A. Fabrication of the body and caps

The 3D-printed valve incorporates a cylindrical body with an integrated membrane, constructed using Filaflex 60A and Ninjaflex 85A filaments on the MK3S printer. The Filaflex 60A filament enables actuation at a lower pressure of 150 kPa, in contrast to the 220 kPa required for Ninjaflex 85A, leading to the selection of Filaflex 60A for the valve body to minimize control pressure. Both filaments are suitable for printing the caps, which are designed to support bottom-inserted tubing and ensure a secure press-fit connection to the valve body, enhanced by an adhesive sealant.

B. Fabrication of 3D printed tubing

We used a desktop FDM printer (Prusa MK3S) with a 0.4 mm nozzle diameter and 0.1 mm layer thickness to fabricate tubing in both horizontal and vertical orientations (**Figure 4A**). An hourglass-shaped design was chosen due to its precise kinking location. Vertically printed tubing in the 3D printed valve underwent layer separation when bent due to weak layer bonding, resulting in failure after ten actuation cycles. In contrast, horizontally printed tubing exhibited a staircase effect due to surface roughness, leading to minor leakage during kinking. Although we succeeded in creating operational valves with tubing printed in both horizontal and vertical orientations, the reliability was low, with only one in five devices functioning properly and a lifespan restricted to less than ten actuation cycles.

C. Our custom nozzle

To address the limitations in FDM's layer-based tube construction, we engineered a custom 3D printer nozzle

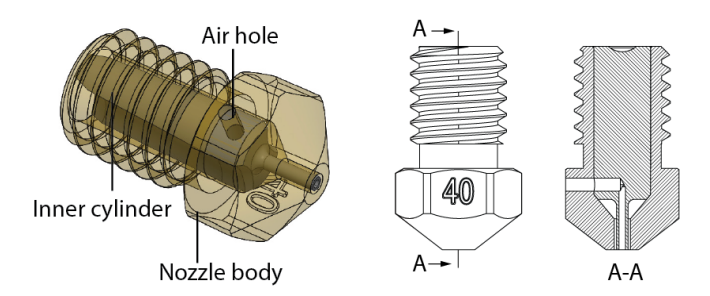


Fig. 5. **Our custom nozzle**. A 3D model of a tube-extruding nozzle including a schematic and a cross-sectional view.

specifically designed for extruding tubes. The internal construction of the nozzle allows for direct isotropic extrusion of thermoplastic materials in tubular geometries [21]. This effectively circumvents the need for layer-stacking used in conventional FDM printing (**Figure 5**). In the absence of additive-layer bonding, the tubes display material characteristics similar to that of the unprocessed filament, notably improved airtightness and enhanced structural integrity under bending stress. Utilizing this specific nozzle, the tubes are fabricated through a single, continuous homogeneous extrusion, either suspended in the air or laid horizontally on the printer's build platform.

The nozzle comprises an inner cylinder and a nozzle body, the latter mimicking the geometry of a conventional "E3D V6" 1 mm nozzle but featuring an additional venting hole on the side. The inner cylinder, a press-fit insert, allows for hollow extrusion patterns by directing molten plastic around a needle at the extrusion end. This needle incorporates an air channel into the venting hole, facilitating air ingress into the emerging hollow tube and precluding vacuum formation within the extruded structure. In this use, any airflow through the nozzle was passively generated from this vacuum.

D. Fabrication of 3D extruded tubing

Our custom nozzle achieves the isotropic extrusion of a tubular structure, which has an inner diameter of $0.7\ mm$ and an outer diameter of $1\ mm$ (Figure 4B). Due to the standard threading equivalent to an E3D nozzle, our custom nozzle can be used on standard FDM printers. We used a *Prusa Mini+* FDM printer (\$399) and the open-source *Pronterface* software to control the printer. To extrude the tubes, we use G-code commands to configure the print parameters and initiate the tubing extrusion process. Using Ninjaflex 85A, we set the nozzle temperature to 235 °C at 100% fan speed and extruded $100\ mm$ of filament.

We extruded tubes from multiple materials, settling on Ninjaflex 85A for optimal performance. Post-extrusion, we adhered to specific geometrical values as described on our GitHub page. Our study covered different material properties and kinking behaviors specific to circular tubes.

E. Assembly of the 3D printed valve

The assembly process of our 3D printed valve requires a valve body along with two end caps and extruded tubing (**Figure 6A**). First, we analyze the tubing to verify

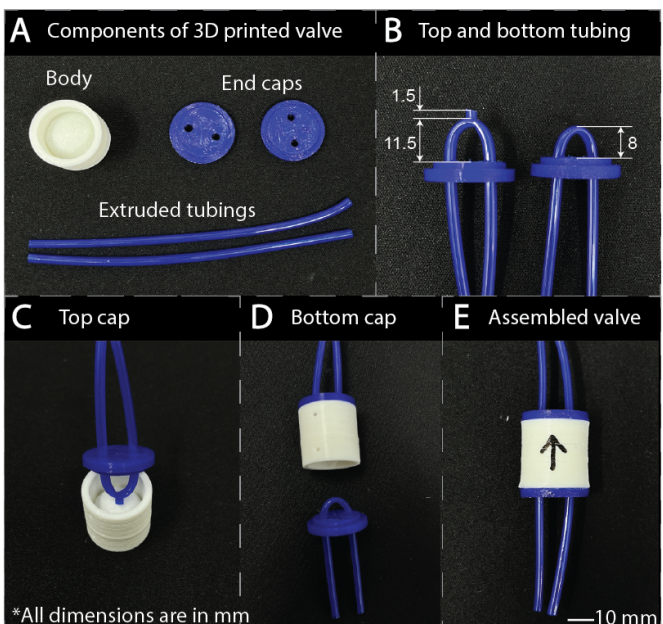


Fig. 6. The assembly process of the 3D printed valve. (A) Photographs of all components required to assemble the valve (B) The top tubing of 11.5 mm length along with 1.5 mm spacer and the bottom tubing of 8 mm are inserted through the holes of caps and sealed. (C) The top cap is press-fitted and sealed to the top part of the membrane and (D) the bottom cap is sealed from other end of the body. (E) A fully assembled 3D printed valve.

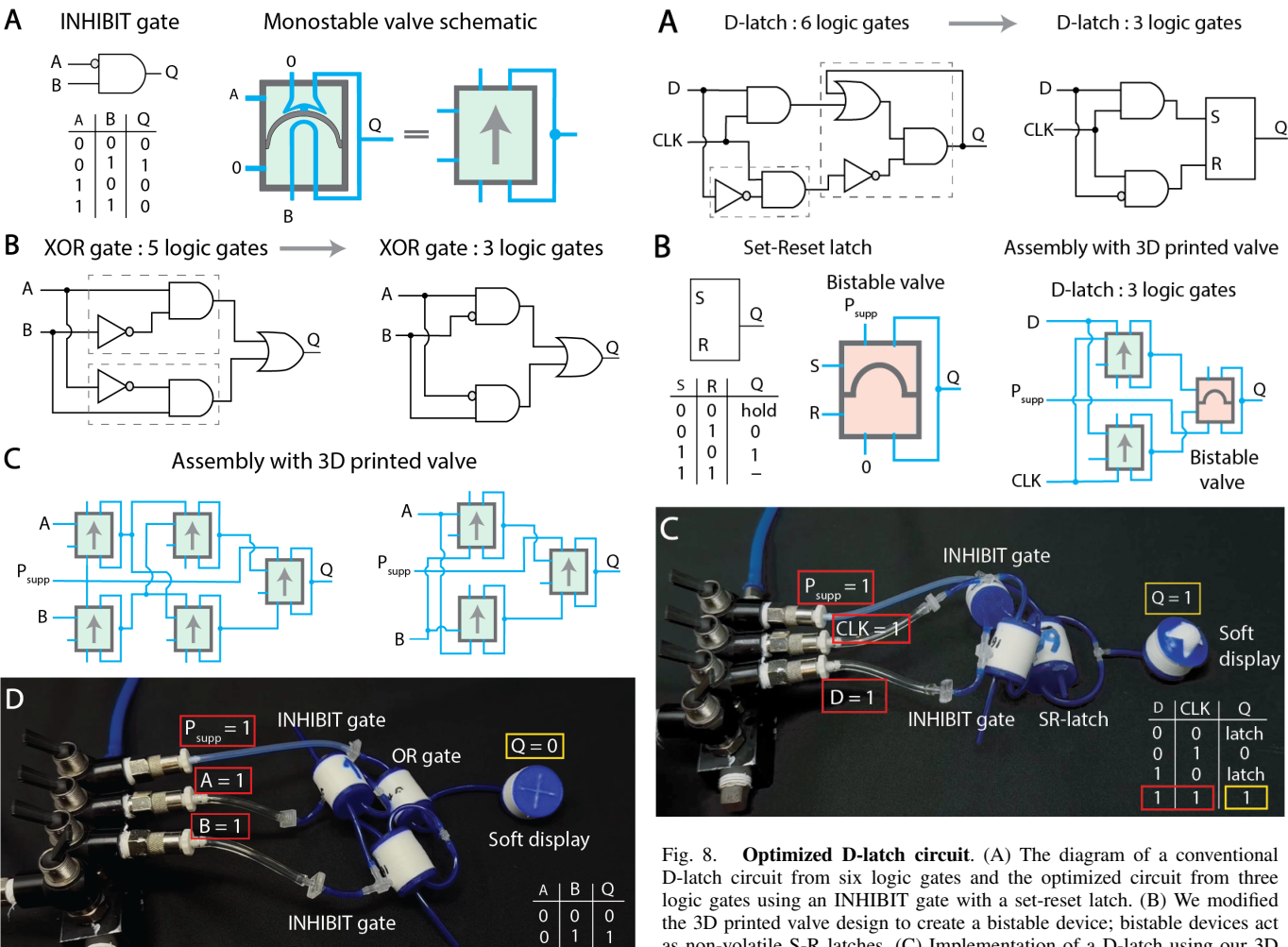
isotropic extrusion and ensure constant thickness. For varied thickness, we place the thicker side of the tube inward to minimize the risk of self-induced kinking. We insert the top (11.5 mm) and bottom tubing (8 mm) through the holes of the end cap, forming an U-shape, and apply adhesive sealant to the connection points (Loctite instant adhesive glue) (Figure 6B). The tube lengths are chosen based on travel distance of the membrane in its deformed state. We glue a 1.5 mm piece of tubing (as a spacer) to the top tubing. Once the tubing is attached and sealed to the end caps, we assemble both caps to the body using more adhesive (Figure 6C and 6D). We also apply adhesive to the outer connections to accomplish an airtight system-level seal (Figure 6E). The assembly protocol along with our .stl files of the 3D printed valve are on our GitHub repository (https://github.com/roboticmaterialsgroup/3D-printed-valve).

III. DEMONSTRATIONS

The soft fluidic valve can be configured into different logic gates and circuits as described in previous papers [8], [10]. Similarly, with our 3D printed design, we configure the valve into NOT-, OR-, and AND-gates. These gates are further stacked to implement increasingly complex fluidic circuits.

A. INHIBIT and XOR gates

The 3D printed valve can be configured as an INHIBIT gate, which integrates NOT- and AND-gate operations. By connecting input A to the top chamber and input B to the bottom tubing, the valve outputs Q=1 only under the condition A=0 and B=1 (**Figure 7A**). In the schematic of



1 1 0

Fig. 7. Optimized XOR gate. (A) An INHIBIT gate along with the truth table and schematic representation. (B) The circuit diagram of a XOR gate with five logic gates. When we optimise the XOR gate using an INHIBIT gate, we only require three logic gates. (C) The assembly of a XOR gate from our 3D printed valves. (D) Implementation of an optimized XOR gate with the output directly connected to a soft display. When both inputs of the XOR gate are HIGH (A = 1 and B = 1), the output is LOW (Q = 0).

INHIBIT gate

INHIBIT gate, the green color highlights a monostable valve design and an arrow indicates position of the membrane. In traditional XOR gate configuration, five logic elements - comprising two NOT gates, two AND gates, and an OR gate - are necessitated. Our work employs an INHIBIT gate to optimize the XOR gate architecture, reducing the required logic gates to three devices only (Figure 7B and 7C). Using a printed version of our previously published, silicone-based soft display [10], we visualized output Q = 0 for inputs A = 1 and B = 1 (Figure 7D).

B. Optimized D-latch circuit

The D-latch, essential in digital systems for data storage and signal synchronization, operates based on two inputs: data (D) and clock (CLK) signals. The output (Q) becomes HIGH(Q = 1) only when both D and CLK are HIGH(D = 1)

D-latch circuit from six logic gates and the optimized circuit from three logic gates using an INHIBIT gate with a set-reset latch. (B) We modified the 3D printed valve design to create a bistable device; bistable devices act as non-volatile S-R latches. (C) Implementation of a D-latch using our 3D printed valves and a soft display. When both the data and clock inputs are HIGH (D = 1 and CLK = 1), the output turns HIGH (Q = 1).

1, CLK = 1). If the CLK signal is LOW (CLK = 0), the output retains its prior state, irrespective of the D input. When D is LOW and CLK is HIGH (D = 0, CLK = 1), the output becomes LOW (Q = 0). This mechanism enables the D-latch to store information.

In traditional D-latch circuits, six logic gates are required: two NOT gates, three AND gates, and an OR gate. Using the INHIBIT gate alongside our bistable valve, we can optimize the circuit to only three logic gates (Figure 8A). The Set-Reset (S-R) latch, a component of the D-latch device, typically uses three logic gates (1 NOT-, 1 AND-, and 1 OR-gate). As we demonstrated previously, the siliconebased soft fluidic valve can be modified to act as a one-bit, non-volatile memory element [10]. In this work, we replace conventional logic gates with an INHIBIT gate and a 3Dprinted bistable valve (memory element), reducing the total gate count from five to three. We show the implementations of both monostable and bistable valve design in a circuit (Figure 8B). We verified the D-latch function using a soft display, confirming that when both D and CLK are HIGH (D=1,CLK=1), the output is HIGH (Q=1) (Figure **8C**).

IV. DISCUSSION

A. 3D printing flexible filaments

FDM printing has limitations, particularly with soft filaments, due to the risk of filament buckling. To mitigate this risk, we employed a Bondtech extruder, enhancing filament feeding and reducing filament slippage due to it's dual-drive system and increased gear reduction ratio. Our elastomeric filaments are highly hydrophilic; we dried them for four hours at $80\,^{\circ}C$ to avoid print defects due to water evaporation at the print nozzle. We printed all devices at a speed of $20\,$ mm/s and a flow rate of 110% to improve airtighness. While we used a TPU of shore hardness 60A, alternatives include Filaflex 70A, Chinchilla 75A, Ninjaflex Edge 83A, and Ninjaflex 85A. A rise in shore hardness directly correlates with elevated control pressures required to operate the 3D-printed valve.

B. Performance of off-the-shelf, extruded, and 3D printed tubing

Among the options of off-the-shelf, molded, or 3D printed tubing for our valve, we opted for 3D printed extruded tubing. Although industrial or molded tubing might offer superior performance in certain respects, our primary objectives were to decrease fabrication time, enable customization through geometrical parameters, and expand the range of printable materials. This approach not only showcases the feasibility of 3D printed extruded tubing but also advances the development of fully 3D printed valves on budgetfriendly printers, thereby enhancing the rapid prototyping capabilities for fluidic circuits.

V. CONCLUSIONS

We investigated the use of FDM printing to fabricate fluidic valves and circuits for soft robotic systems. We show the reduction of the fabrication time of the soft fluidic valve from 27 hours with replica molding to 3 hours with FDM printing. By parallelizing FDM printers, the prototyping and fabrication of fluidic circuits can be accelerated further. Our innovative custom nozzle enables tube extrusion on standard FDM printers. We optimized XOR gate and D-latch circuits to three logic gates each, utilizing both mono- and bi-stable fluidic valves. Overall, FDM printing emerges as a low-cost approach for the widespread dissemination and adoption of fluidic control elements within the broader academic community.

REFERENCES

- [1] G. M. Whitesides, "Soft robotics," *Angewandte Chemie International Edition*, vol. 57, no. 16, pp. 4258–4273, 2018.
- [2] J. Walker, T. Zidek, C. Harbel, S. Yoon, F. S. Strickland, S. Kumar, and M. Shin, "Soft robotics: A review of recent developments of pneumatic soft actuators," *Actuators*, vol. 9, no. 1, 2020.
- [3] S. Huang, Y. Liu, Y. Zhao, Z. Ren, and C. F. Guo, "Flexible electronics: Stretchable electrodes and their future," *Advanced Functional Materials*, vol. 29, no. 6, p. 1805924, 2019.
- [4] M. Wehner, R. L. Truby, D. J. Fitzgerald, B. Mosadegh, G. M. Whitesides, J. A. Lewis, and R. J. Wood, "An integrated design and fabrication strategy for entirely soft, autonomous robots," *Nature*, vol. 536, no. 7617, pp. 451–455, 8 2016.

- [5] J. D. Hubbard, R. Acevedo, K. M. Edwards, A. T. Alsharhan, Z. Wen, J. Landry, K. Wang, S. Schaffer, and R. D. Sochol, "Fully 3d-printed soft robots with integrated fluidic circuitry," *Science Advances*, vol. 7, no. 29, p. eabe5257, 2021.
- [6] P. Rothemund, A. Ainla, L. Belding, D. J. Preston, S. Kurihara, Z. Suo, and G. M. Whitesides, "A soft, bistable valve for autonomous control of soft actuators," *Science Robotics*, 2018.
- [7] S. V. Kendre, L. Whiteside, T. Y. Fan, J. A. Tracz, G. T. Teran, T. C. Underwood, M. E. Sayed, H. J. Jiang, A. A. Stokes, D. J. Preston, G. M. Whitesides, and M. P. Nemitz, "The Soft Compiler: A Web-Based Tool for the Design of Modular Pneumatic Circuits for Soft Robots," *IEEE Robotics and Automation Letters*, vol. 7, no. 3, pp. 6060–6066, 7 2022.
- [8] D. J. Preston, P. Rothemund, H. J. Jiang, M. P. Nemitz, J. Rawson, Z. Suo, and G. M. Whitesides, "Digital logic for soft devices," Proceedings of the National Academy of Sciences of the United States of America, vol. 116, no. 16, pp. 7750–7759, 4 2019.
- [9] D. J. Preston, H. J. Jiang, V. Sanchez, P. Rothemund, J. Rawson, M. P. Nemitz, W.-K. Lee, Z. Suo, C. J. Walsh, and G. M. Whitesides, "A soft ring oscillator," *Science Robotics*, 2019.
- [10] M. P. Nemitz, C. K. Abrahamsson, L. Wille, A. A. Stokes, D. J. Preston, and G. M. Whitesides, "Soft non-volatile memory for non-electronic information storage in soft robots," in 2020 3rd IEEE International Conference on Soft Robotics (RoboSoft), 2020, pp. 7–12
- [11] D. Drotman, S. Jadhav, D. Sharp, C. Chan, and M. T. Tolley, "Electronics-free pneumatic circuits for controlling soft-legged robots," *Science Robotics*, vol. 6, no. 51, p. eaay2627, 2021.
- [12] J. A. Tracz, L. Wille, D. Pathiraja, S. V. Kendre, R. Pfisterer, E. Turett, C. K. Abrahamsson, S. E. Root, W. K. Lee, D. J. Preston, H. J. Jiang, G. M. Whitesides, and M. P. Nemitz, "Tube-Balloon Logic for the Exploration of Fluidic Control Elements," *IEEE Robotics and Automation Letters*, vol. 7, no. 2, pp. 5483–5488, 4 2022.
- [13] C. J. Decker, H. J. Jiang, M. P. Nemitz, S. E. Root, A. Rajappan, J. T. Alvarez, J. Tracz, L. Wille, D. J. Preston, and G. M. Whitesides, "Programmable soft valves for digital and analog control," *Proceedings of the National Academy of Sciences*, vol. 119, no. 40, p. e2205922119, 2022.
- [14] W.-K. Lee, D. J. Preston, M. P. Nemitz, A. Nagarkar, A. K. MacKeith, B. Gorissen, N. Vasios, V. Sanchez, K. Bertoldi, L. Mahadevan, and G. M. Whitesides, "A buckling-sheet ring oscillator for electronicsfree, multimodal locomotion," *Science Robotics*, vol. 7, no. 63, p. eabg5812, 2022.
- [15] A. Rajappan, B. Jumet, R. A. Shveda, C. J. Decker, Z. Liu, T. F. Yap, V. Sanchez, and D. J. Preston, "Logic-enabled textiles," *Proceedings of the National Academy of Sciences*, vol. 119, no. 35, p. e2202118119, 2022.
- [16] Q. Lu, H. Xu, Y. Guo, J. Y. Wang, and L. Yao, "Fluidic computation kit: Towards electronic-free shape-changing interfaces," in *Proceed*ings of the 2023 CHI Conference on Human Factors in Computing Systems, ser. CHI '23. New York, NY, USA: Association for Computing Machinery, 2023.
- [17] S. Song, S. Joshi, and J. Paik, "CMOS-Inspired Complementary Fluidic Circuits for Soft Robots," *Advanced Science*, vol. 8, no. 20, 10 2021.
- [18] S. Wang, L. He, and P. Maiolino, "Design and characterization of a 3d-printed pneumatically-driven bistable valve with tunable characteristics," *IEEE Robotics and Automation Letters*, vol. 7, no. 1, pp. 112–119, jan 2022.
- [19] Y. Zhai, A. D. Boer, J. Yan, B. Shih, M. Faber, J. Speros, R. Gupta, and M. T. Tolley, "Desktop fabrication of monolithic soft robotic devices with embedded fluidic control circuits," *Science Robotics*, vol. 8, no. 79, p. eadg3792, 2023.
- [20] J. V. Chen, A. B. Dang, and A. Dang, "Comparing cost and print time estimates for six commercially-available 3d printers obtained through slicing software for clinically relevant anatomical models," 3D Printing in Medicine, vol. 7, no. 1, 2021.
- [21] E. Wilke, "Nozzle for printing tubes," US patent application: 63/434,503, 2023.